



# Reaction dynamics of $\text{Mg}(3^1\text{P}_1, 4^1\text{S}_0)$ with $\text{H}_2$ : insertion versus harpoon mechanism

Dean-Kuo Liu, King-Chuen Lin \*

*Department of Chemistry, National Taiwan University, and Institute of Atomic and Molecular Sciences, Academia Sinica, Taipei 10764, Taiwan, Republic of China*

Received 1 March 1997; in final form 12 May 1997

## Abstract

We have obtained nascent rotational distributions of  $\text{MgH}$  ( $v = 0$  and  $1$ ) in the reaction of  $\text{Mg}(4^1\text{S}_0)$  with  $\text{H}_2$ . The resultant bimodal features of the  $\text{MgH}$  distributions are similar to those obtained from  $\text{Mg}(3^1\text{P}_1)$ . The spectral analysis and potential energy surfaces calculation suggest that the  $\text{Mg}(4^1\text{S}_0)$  atom proceeds via a harpoon-type reaction pathway, in contrast to a direct insertion followed by  $\text{Mg}(3^1\text{P}_1)$ . The  $\text{Mg}(4^1\text{S}_0)$  system is closely associated with the  $\text{Mg}(3^1\text{P}_1)$ – $\text{H}_2$  reaction coordinate, through evolution of a series of surface crossings along the ion-pair coordinate. © 1997 Elsevier Science B.V.

## 1. Introduction

The reaction dynamics of  $\text{Mg}(3s3p^1\text{P}_1)$  with  $\text{H}_2$  has been well studied more than a decade [1–7]. The produced nascent  $\text{MgH}$  exhibits a bimodal rotational distribution. The insertion mechanism is found to be the only channel that causes the bimodality, in the light of the measurements of isotope and temperature effects on the  $\text{MgH}$  distribution [2,3]. Potential energy surfaces (PES) calculation also indicates that the reactive coordinate along the  $^1\text{B}_2$  surface in  $\text{C}_{2v}$  geometry is attractive, while the collinear approach suffers from a substantial energy barrier [6]. Our recent study of a two-dimensional PES calculation reveals that the reactive surface of the excited state

crosses non-adiabatically to the ground state, on which the  $\text{MgH}_2$  intermediate complex begins to break apart through two possible trajectories leading to the  $\text{MgH}(^2\Sigma^+)$  and  $\text{H}$  products [8,9]. A corresponding quasiclassical trajectory calculation lends support to the above prediction [9].

By analogy with the  $\text{Mg}(^1\text{P}_1)$ – $\text{H}_2$  reaction, Kleiber and coworkers in a study of  $\text{Na}(4p)$  reaction with  $\text{H}_2$  found a similar rotational bimodality of the  $\text{NaH}$  product [10,11]. The bimodal nature was anticipated primarily to stem from a side-on attack along an attractive surface, which determined the microscopic branching late in the exit channel. In contrast, the reactions of excited  $\text{K}$  or  $\text{Cs}$  with  $\text{H}_2$  are dominated by a harpoon mechanism [12–14]. As the alkali atom approaches collinearly to some distance,  $\text{K}$  or  $\text{Cs}$  eject an electron to the  $\text{H}_2$  molecule, and then the  $\text{H}$  atom flies apart from the ion-pair intermediate. Due to the instability of  $\text{H}_2^-$ , the resulting

\* Corresponding author. Fax: 886-2-3636359, e-mail: kclin@hp9k720.iams.sinica.edu.tw.

product energy disposal is predominantly partitioned into translation [13]. Bersohn and coworkers suggested that the size of alkali elements may be an important factor to determine the mechanism preference [14]. Such a competition of insertion versus harpoon-type mechanism has also been found in the alkaline earth atom with OH-containing molecules [15,16]. The former pathway proceeds via a long-lived intermediate complex, which then evolves to different product channels, whereas the latter one forms only the metal hydroxide product.

From the energetic point of view, the ionization potential of the metal element is lowered by the electronic excitation, and thereby the rate of electron transfer is enhanced. In this note, we look into such an effect of excitation energy on the reaction mechanisms of Mg(3p) and Mg(4s) plus H<sub>2</sub> collisions. The ionization potential of Mg(4s) is lowered relative to Mg(3p) by 1.1 eV.

## 2. Experiment

A similar experimental apparatus with a pump-probe technique has been illustrated in detail elsewhere [1–5,7], so only a brief description is given here. Two dye lasers, each pumped by an individual Nd:YAG laser, were employed as the radiation sources. The pump laser was operated to emit at 459.7 nm for excitation of Mg(4s) by two-photon absorption. After a brief time delay of less than 10 ns, the probe laser was fired to monitor the laser-induced fluorescence (LIF) spectra of the resulting MgH product in the A<sup>2</sup>Π–X<sup>2</sup>Σ<sup>+</sup> band. The laser energies of both lasers were adjusted to avoid optical saturation or unwanted multiphoton excitation.

The Mg metal, deposited in a five-armed cross heat-pipe oven, was heated to 750–760 K, corresponding to a vapor pressure of 40–50 mTorr. The pressure of H<sub>2</sub> in the oven was maintained at less than 4 Torr to allow for the MgH produced to be detected in a nascent state.

## 3. Results and discussion

The obtained LIF spectra of MgH (*v* = 0 and 1) between Mg(4s) and Mg(3p) are very similar. Taking

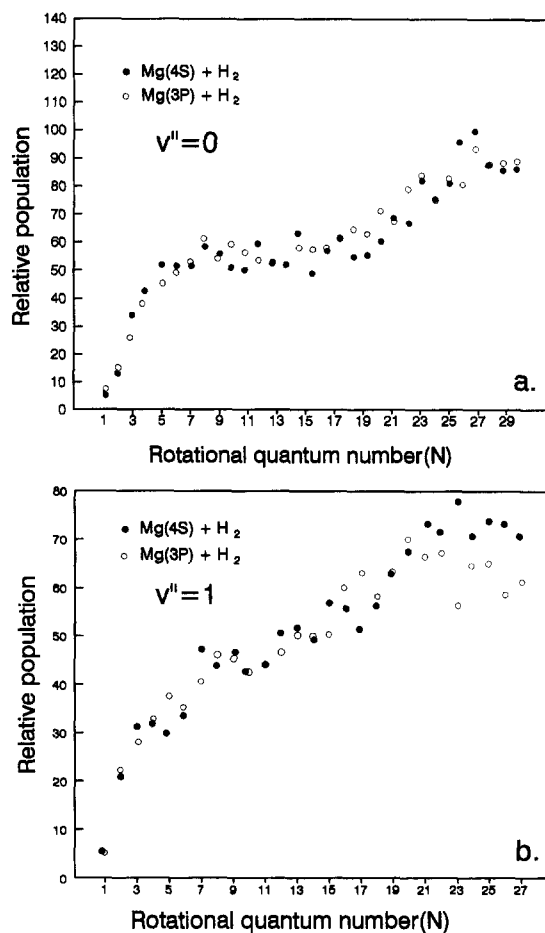


Fig. 1. Comparison of the rotational distributions of MgH(*v* = 0 and 1) resulting from Mg(3<sup>1</sup>P<sub>1</sub>) and Mg(4<sup>1</sup>S<sub>0</sub>).

into account the Hönl–London factor and intensity correction for the low-*N* component (*N* ≤ 5) [7], we found that the normalized MgH (*v* = 0 and 1) rotational distributions obtained from Mg(4s) are essentially consistent with those from Mg(3p), except for a few high-*N* lines in the (0,1) band. The comparison of MgH distributions, represented by the P<sub>1</sub> branch, is shown in Fig. 1. Note that a computer simulation was applied to resolve the spectra around the band head. (The *N* = 11–20 lines for the (0,0) band and *N* = 8–14 lines for the (0,1) band [7].)

One should be cautious in studying a reaction initiated by a highly excited atom that electronic relaxation is negligible, i.e. that lower states populated by relaxation do not form the same product to interfere with the study. We examine the probability

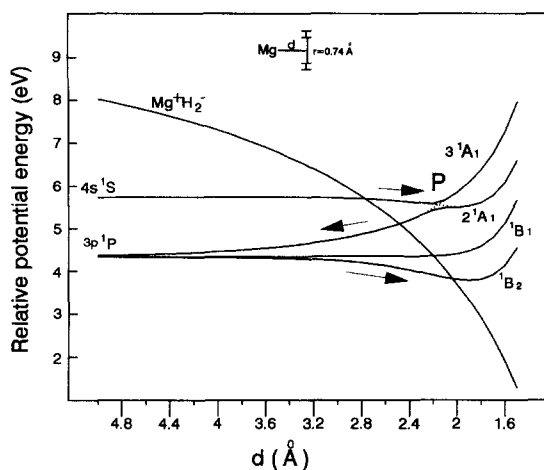


Fig. 2. Calculation of potential energy surfaces as a function of internuclear distance.

of product contribution by these states through collisional and radiative relaxation. Since the obtained MgH is in a nascent state, the product contribution associated with the process of collisional relaxation is negligible under our experimental conditions. The radiative relaxation for the  $4s \rightarrow 3p$  transition gives rise to a spontaneous emission coefficient of  $2.6 \times 10^7 \text{ s}^{-1}$ , corresponding to a lifetime of 39 ns. During the delay time adopted, a  $< 25\%$  population contribution of MgH may result from the relaxed  $3p$  state. In fact, we have shortened the delay time, but the obtained bimodal feature of the MgH distributions does not show any significant change.

To provide insight into the reaction pathway associated with the Mg( $4s$ ) state, we present in Fig. 2 the potential energies of Mg( $3p$ ,  $4s$ )- $\text{H}_2$  reactions as a function of the internuclear distance in a  $C_{2v}$  symmetry. The calculations were done using basis sets in  $6-31G^{**}$  level for the Mg and H atoms. Configuration interaction calculations with single excitation (CIS) contained in the GAUSSIAN 92 package were used for the computation. The  $^1P_1$  state is splitted into three surfaces ( $2^1A_1$ ,  $^1B_1$  and  $^1B_2$ ) as Mg and  $\text{H}_2$  approach. The corresponding PESs are consistent with those computed by Chaquin and coworkers [6]. At an internuclear distance about  $2.2 \text{ \AA}$ , the repulsive  $2^1A_1$  curve has an avoided crossing with the upper  $3^1A_1$  curve, which correlates with the  $4^1S_0$  state.

The potential diagram for the Mg( $3p$ ,  $4s$ )- $\text{H}_2$  reaction is found to be similar to that in the Na( $3p$ ,

$4s$ )- $\text{H}_2$  reaction [17]. Therefore, we propose a reaction pathway for the Mg( $4s$ ) system analogous to the Na- $\text{H}_2$  case [10,11,17]. The Mg( $4s$ )- $\text{H}_2$  collision begins to go along the attractive  $3^1A_1$  surface, and then crosses to the  $2^1A_1$  surface. The  $4s$  state, which lies close to the ionization continuum, gains more ionic character than the  $3p$  state. The mixing of valence and partial ionic characters allows for a certain probability for the non-adiabatic transition. For jumping to the reactive  $^1B_2$  surface, Mg and  $\text{H}_2$  have to fly apart to the vicinity of the asymptotic  $3p$  state. Finally, the Mg- $\text{H}_2$  tracks along the  $^1B_2$  surface, leading to a similar rotational distribution as in the  $3p$  state reaction. An analogous interpretation has been applied to the Na( $4s$ ,  $4p$ )- $\text{H}_2$  reactions [10,11,17]. However, here the probability for curve crossing from  $2^1A_1$  to  $^1B_2$  is questionable. Since a large repulsive force is exerted on the Mg- $\text{H}_2$  intermediate as it tracks along  $2^1A_1$ , the moiety should break apart rapidly to Mg( $3p$ ) plus  $\text{H}_2$ . A secondary collision of Mg( $3p$ ) seems to be required to produce MgH.

In the following we propose an alternative mechanism to proceed via a harpoon-type pathway. An ion-pair curve, dominated by the Coulombic force, is included in the potential diagram of Fig. 2. The electron affinity of  $\text{H}_2$  is adopted as  $-2.1 \text{ eV}$ . As Mg( $4s$ ) approaches towards  $\text{H}_2$ , a series of non-adiabatic curve crossings are found along the  $\text{Mg}^+\text{H}_2^-$  coordinate, and including finally one to the reactive  $^1B_2$  surface. Note that the crossing region lies in the attractive entrance channel of  $^1B_2$  about  $2 \text{ \AA}$  prior to crossing to the ground state surface, where the anisotropy causes the bimodal nature of the rotational distribution. The similarity of the corresponding MgH distributions obtained by  $3^1P_1$  and  $4^1S_0$  is indicative of two things. First, the Mg( $4s$ ) collision by  $\text{H}_2$  is closely associated with the Mg( $3p$ )- $\text{H}_2$  reaction coordinate through evolution of a series of surface crossings. Second, the product energy disposal in the Mg( $4s$ ) reaction, which has  $1.1 \text{ eV}$  more excitation energy than the  $3p$  state, is dominated by translation. In the process of electron transfer, the strong instability of  $\text{H}_2^-$  tends to cause most of the energy to be partitioned into translation [13]. Unlike the case of the  $3p$  state, the excitation energy facilitates the Mg( $4s$ ) plus  $\text{H}_2$  reaction via the pathway of electron transfer, rather than by

formation of a stable insertive intermediate complex. By analogy with our work, in the reactions of  $\text{Ca}(^1\text{S}_0, ^3\text{P}_j)$  with  $\text{H}_2\text{O}_2$ , the  $\text{Ca}(^3\text{P}_j)$  state produces  $\text{CaOH}$ , while the ground state atom leads to only  $\text{CaO}$  [16]. The corresponding pathways proceed along an insertion either into an O–O or an O–H bond. A competition occurs between dissociation of the intermediate complex and migration of the H atom. The reaction with  $\text{Ca}(^3\text{P}_j)$  is ascribed to an electron transfer, such that the ion-pair intermediate formed has no time to allow for H atom migration prior to dissociation.

In summary, the analysis of  $\text{MgH}$  rovibrational spectra suggests that the  $\text{Mg}(4^1\text{S}_0)$  atom proceeds via a harpoon-type reaction pathway, in contrast to a direct insertion mechanism for the  $\text{Mg}(3^1\text{P}_1)$  plus  $\text{H}_2$  reaction. The competition of electron transfer versus insertion depends on excitation energy. As the excitation energy increases, the harpoon process is favored, through which the reaction coordinate is joined to the reactive  $^1\text{B}_2$  surface.

### Acknowledgements

This work is supported by the National Science Council, the Republic of China, under the contract No. NSC86-2113-M001-044-L2.

### References

- [1] W.H. Breckenridge, H. Umemoto, *J. Chem. Phys.* 80 (1984) 4168.
- [2] W.H. Breckenridge, J.H. Wang, *Chem. Phys. Lett.* 82 (1985) 4945.
- [3] K.C. Lin, C.T. Huang, *J. Chem. Phys.* 91 (1989) 5387.
- [4] P.D. Kleiber, A.M. Lyyra, K.M. Sando, S.V. Zafirooulos, W.C. Stwalley, *J. Chem. Phys.* 85 (1986) 5493.
- [5] P.D. Kleiber, A.M. Lyyra, K.M. Sando, S.P. Heneghan, W.C. Stwalley, *Phys. Rev. Lett.* 54 (1985) 2003.
- [6] P. Chaquin, A. Sevin, H. Yu, *J. Phys. Chem.* 89 (1985) 2813.
- [7] D.K. Liu, T.L. Chin, K.C. Lin, *Phys. Rev. A* 50 (1994) 4891.
- [8] D.K. Liu, T.L. Chin, Y.R. Ou, C.T. Huang, K.C. Lin, *J. Chin. Chem. Soc.* 42 (1995) 293.
- [9] Y.R. Ou and K.C. Lin (to be published).
- [10] S. Bililign, P.D. Kleiber, W.R. Kearney, K.M. Sando, *J. Chem. Phys.* 96 (1992) 218.
- [11] S. Bililign, P.D. Kleiber, *J. Chem. Phys.* 96 (1992) 213.
- [12] A.G. Urena, R. Vetter, *Int. Rev. Phys. Chem.* 15 (1996) 375.
- [13] D.K. Liu, K.C. Lin, *J. Chem. Phys.* 105 (1996) 9121.
- [14] X. Huang, J. Zhao, G. Xing, X. Wang, R. Bersohn, *J. Chem. Phys.* 104 (1996) 1338.
- [15] P. de Pujo, O. Sublementier, J.P. Visticot, J. Berlande, J. Cuvelier, C. Alcaraz, T. Gustavsson, J.M. Mestdagh, P. Meynadier, *J. Chem. Phys.* 99 (1993) 2533.
- [16] M.D. Oberlander, R.P. Kampf, J.M. Parson, *Chem. Phys. Lett.* 176 (1991) 385.
- [17] A. Sevin, P. Chaquin, *Chem. Phys.* 93 (1985) 49.